

Available online at [www.sciencedirect.com](http://www.sciencedirect.com)

Chinese Journal of Aeronautics 22(2009) 505-512

**Chinese  
Journal of  
Aeronautics**
[www.elsevier.com/locate/cja](http://www.elsevier.com/locate/cja)

## Design and Experiment of PZT Network-based Structural Health Monitoring Scanning System

Qiu Lei, Yuan Shenfang\*, Wang Qiang, Sun Yajie, Yang Weiwei

*The Aeronautic Key Lab for Smart Material and Structure, Nanjing University of Aeronautics and Astronautics, Nanjing 210016, China*

Received 7 October 2008; accepted 23 April 2009

### Abstract

The active Lamb wave and piezoelectric transducer (PZT)-based structural health monitoring (SHM) technology is a kind of efficient approach to estimate the health state of aircraft structure. In practical applications, PZT networks are needed to monitor large scale structures. Scanning many of the different PZT actuator-sensor channels within these PZT networks to achieve on-line SHM task is important. Based on a peripheral component interconnect extensions for instrumentation (PXI) platform, an active Lamb wave and PZT network-based integrated multi-channel scanning system (PXI-ISS) is developed for the purpose of practical applications of SHM, which is compact and portable, and can scan large numbers of actuator-sensor channels and perform damage assessing automatically. A PXI-based 4 channels gain-programmable charge amplifier, an external scanning module with 276 actuator-sensor channels and integrated SHM software are proposed and discussed in detail. The experimental research on a carbon fiber composite wing box of an unmanned aerial vehicle (UAV) for verifying the functions of the PXI-ISS is mainly discussed, including the design of PZTs layer, the method of excitation frequency selection, functional test of damage imaging, stability test of the PXI-ISS, and the loading effect on signals. The experimental results have verified the stability and damage functions of this system.

**Keywords:** structural health monitoring; active Lamb wave; piezoelectric transducer network; multi-channel scanning system; damage detection

### 1. Introduction

Structural health monitoring (SHM) technology is a reliable, efficient and economical approach to increase the safety and reduce the maintenance cost of high performance structures<sup>[1]</sup>. The active Lamb wave and piezoelectric transducer (PZT)-based methods have been studied by many researchers in recent years<sup>[2-8]</sup>. To monitor large-scale structures, the PZT networks are needed. How to scan different PZT actuator-sensor channels within these PZT networks to achieve on-line and stable SHM task is an important issue for good application of these methods.

Traditional PZT-based SHM systems consist of many individual instruments including waveform generator, power amplifier, charge amplifier and computer-based data acquisition system/oscilloscope. These kinds of

monitoring systems are bulky, heavy and inconvenient for channel switching. The instruments in these kinds of systems use different software systems which make the PZT-based methods inconvenient to be applied in practical engineering application. In respect of the scanning system of multi-channel PZT network for SHM, till now, only Acellent Corporation in USA reported that they developed an SHM instrument called smart-suitcase to solve this problem<sup>[9-10]</sup>. But this system was based on an industrial PC and they did not release any details of its development. J. R. Dove, et al.<sup>[11]</sup> developed a relay-based hardware in conjunction with PZT active-sensing technique for SHM. V. Giurgiutiu, et al.<sup>[12-13]</sup> developed a switching unit to control actuator-sensor channels. S. F. Yuan, et al.<sup>[14]</sup> developed an integrated health monitoring scanning system, but the hardware, software and damage assessing function of this system remained to be improved.

This article introduces the development of an active Lamb wave and PZT network-based integrated multi-channel scanning system (ISS) based on a peripheral component interconnect extension for instrumentation (PXI) platform (PXI-ISS) which is compact and portable for the purpose of practical applications of SHM to scan large numbers of PZT actuator-sensor channels,

\*Corresponding author. Tel.: +86-25-84893460.

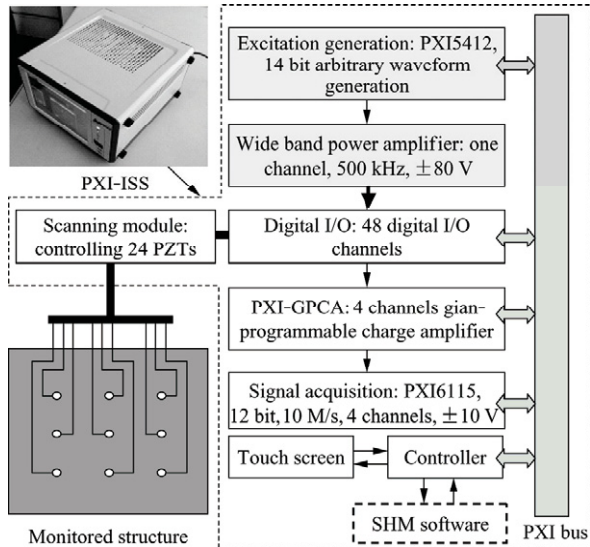
E-mail address: [ysf@buaa.edu.cn](mailto:ysf@buaa.edu.cn)

Foundation items: National High-tech Research and Development Program of China (2007AA03Z117); National Natural Science Foundation of China (50830201); Graduate Education Innovation Project of Nanjing University of Aeronautics and Astronautics of China (BCXJ09-01).

process signals, and assess structural damage automatically. Adopting this system, the SHM experimental research on a wing box is performed which shows that the developed PXI-ISS possesses good performance.

## 2. System Hardware Realization

To have an integrated, stable and portable SHM system, the PXI-ISS presented in this article is designed to be integrated into a PXI platform. The architecture of this PXI-ISS is shown in Fig.1.



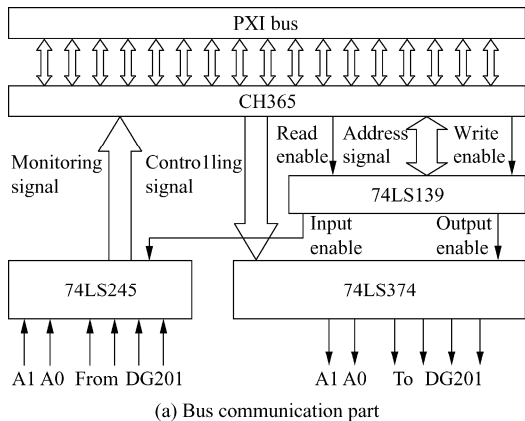
Note: PXI-GPCA—PXI bus-based gain-programmable charge amplifier

Fig.1 Architecture of PXI-ISS.

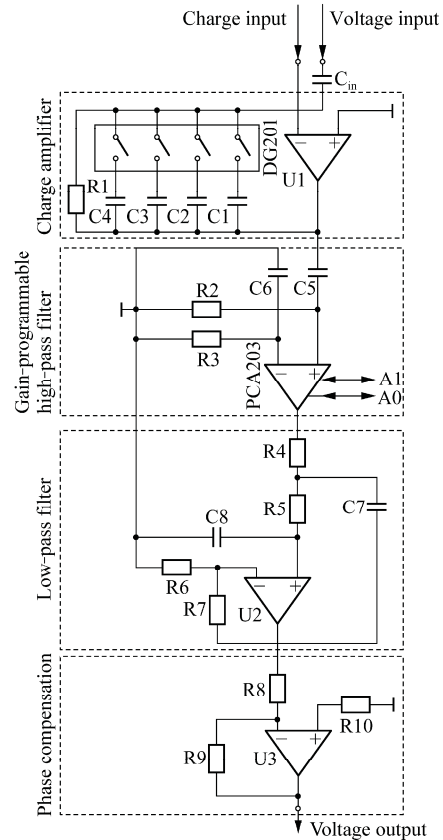
### 2.1. Design of gain-programmable charge amplifier

Since there is no commercially available PXI-GPCA board which can be inserted into industrial computer, a PXI-GPCA board with 4 channels is developed. Its power comes from the  $\pm 12$  V and +5 V power of the PXI bus.

The PXI-GPCA consists of two parts: a signal amplifier part which is used to amplify the response signals and a bus communication part which is used to control the gain and sensitivity of the signal amplifier part. The schematic diagram is shown in Fig.2.



(a) Bus communication part



(b) Signal amplifier part/one channel

Fig.2 Schematic diagram of PXI-GPCA.

The bandwidth of the developed PXI-GPCA is tested using a sine sweeping signal of  $\pm 50$  mV amplitude and 0 Hz to 1 MHz frequency. The gain and sensitivity are set to be at the highest state. The obtained gain/frequency curve is shown in Fig.3. It represents that the  $-3$  dB bandwidth is between 15 kHz and 640 kHz. Considering that the generally used frequency range of active Lamb wave-based methods is between 30 kHz and 400 kHz, this bandwidth is suitable for their applications.

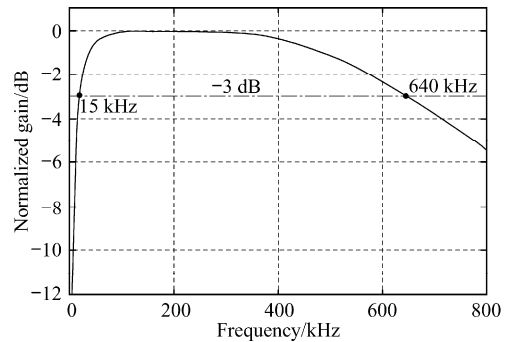


Fig.3 Bandwidth test of PXI-GPCA.

### 2.2. Design of scanning module

A scanning module which consists of two low cross talk switch boards (LCSB) is designed to switch dif-

ferent channels to achieve the scanning function of the PXI-ISS.

The excitation signal sent to a PZT is usually a signal of high amplitude and high frequency, while the response signal of PZT is a signal of small amplitude. In this case, the cross talk between the excitation channel and the sensing channel has to be considered in the design. When the cross talk signal is in a high level, the PXI-GPCA may be saturated so that the response signal can not be amplified normally. If the amplitude of the cross talk signal is higher than the response signal, some features such as the peak value, time-of-flight and energy of the response signal are hardly to be recognized by software automatically.

The designed schematic diagram of the LCSB and its hardware is shown in Fig.4(a). Since the digital I/O board has 24 digital I/O channels and a 12 V voltage power at one digital I/O port, the designed LCSB contains 24 relays, which is controlled and powered by the digital I/O board. The chip of the relay driver is ULN2003. The relay array contains 24 single pole double throw (SPDT) relays of which the model is TIANBO HJR-4102-L-12V. Two LCSBs are adopted. One is connected to the power amplifier for the excitation channels and the other is connected to the PXI-GPCA for the sensing channels. The developed scanning module can be connected with 24 PZTs as shown in Fig.4(b).

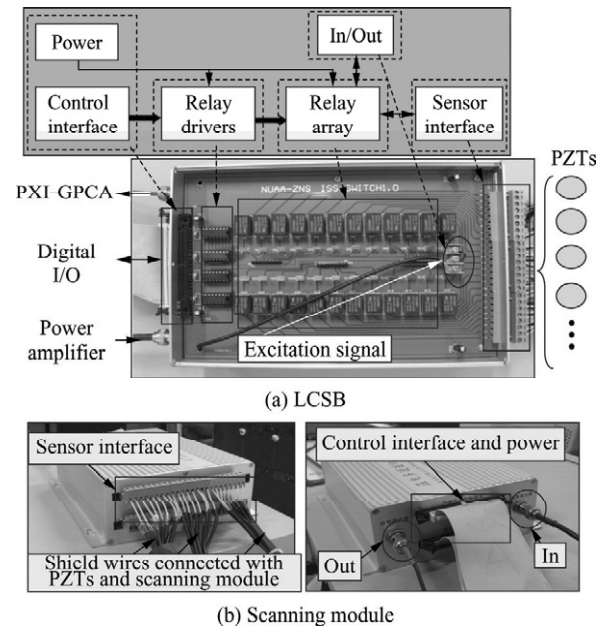


Fig.4 Schematic diagrams and hardware of LCSB and scanning module.

Fig.5 gives a detailed description of the connection method for the scanning module. This kind of connection method can greatly reduce the level of cross talk signals to an acceptable level by making two poles of PZTs be at the low impedance state when they are not working.

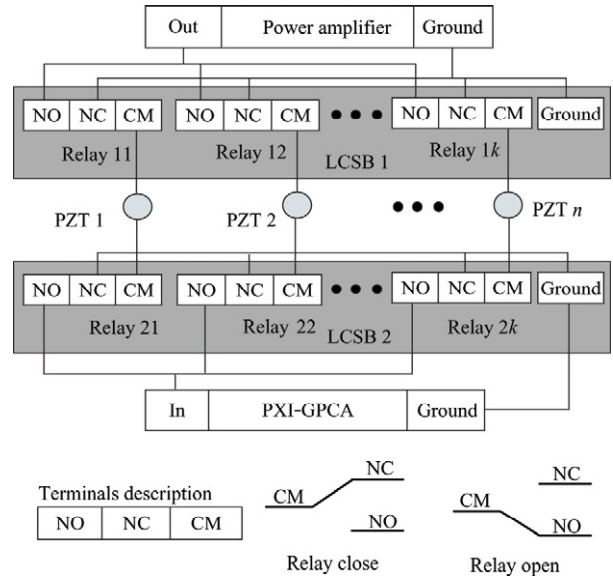
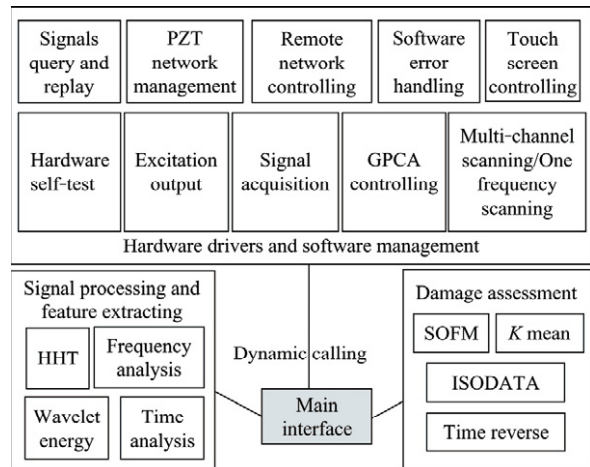


Fig.5 Connection method between PZTs and two LCSBs.

### 3. System Software Realization

Integrated SHM software which is based on the Lab-VIEW software platform is developed to manage the whole hardware, extract damage features and realize damage assessment. Its architecture is shown in Fig.6.



Note: HHT—Hilber Huang transform; ISODATA—Interactive self-organization data; SOFM—Self-organization feature map.

Fig.6 Architecture of software.

The hardware drivers and software management module contains the basic functions including driving different hardware to work orderly, building database to manage acquired signals, and managing PZT network information. The programming techniques including the DAQmx, the dynamic load VI, and the producer and consumer programming model are adopted to improve the running efficiency of this module.

Signal processing and feature extracting module is designed to process the acquired signals and acquire

their features of time, frequency and time-frequency domains. In wavelet energy sub module, the morlet wavelet is adopted to acquire the wavelet energy of response signals. In HHT sub module, the energy of main intrinsic mode functions (IMF) is obtained.

In damage assessment module, time reverse<sup>[15]</sup> method and pattern recognition methods including SOFM neural network, *K* mean and ISODATA cluster method are used to assess the extent and location of damage.

In the last two modules, the C++ shared library calling MATLAB technique is adopted to realize the complicated algorithms of the signal processing, pattern recognition and time reverse method.

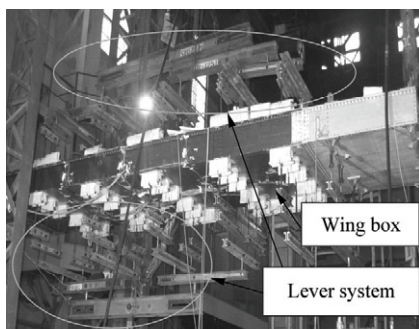
#### 4. Experiment

The experiment using this PXI-ISS is performed in the Aircraft Strength Research Institute of China including the design of PZTs layer, the method of excitation frequency selection, the functional test of damage imaging, the stability test of the PXI-ISS and the loading effect on signals. In the experiment, the functional integrity, especially the multi-channel and frequency scanning and the damage assessment function of the PXI-ISS are verified.

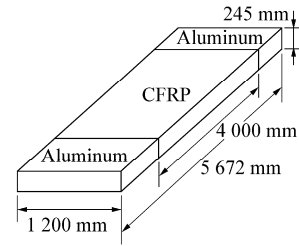
##### 4.1. Wing box specimen and load setup

The main material of wing box is carbon fiber-reinforced polymers (CFRP). The upper and lower panels are laminated plates and wearing patterns are  $[45/0/-45/90/0/-45/0/90/-45/0/45/\bar{0}]$ .

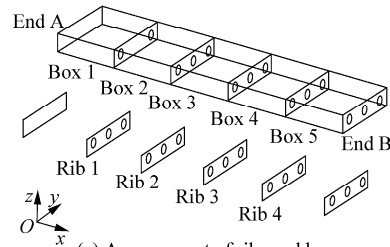
Each layer is 0.16 mm in thickness, so the upper and lower panels are 3.68 mm in thickness. Fig.7 gives the picture, dimensions, arrangement of ribs and boxes, and loading state of the wing box respectively. The dimensions of wing box are 4 000 mm long, 1 200 mm wide and 245 mm thick. A fixed end (called End A) and a freedom end (called End B) which are made of aluminum material are placed on the two sides of wing box. Four ribs named Rib 1 to Rib 4 are placed in wing box which divide it into five wing boxes called Box 1 to Box 5. The upper panel is connected with the four ribs using adhesive bonding and rib-bolts.



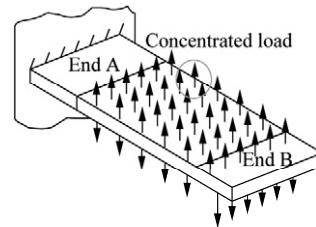
(a) Wing box specimen



(b) Dimensions



(c) Arrangement of ribs and boxes



(d) Loading condition

Fig.7 Illustration of wing box.

The design load is a static bending moment and is applied to the wing box in the form of concentrated load through a lever system as shown in Fig.7(a). The ultimate value of the bending moment is 63.9 kN·m. In the experiment, the maximum bending moment applied to wing box is 60% of its ultimate value. The loading process is divided into eight steps which are 0%, 10%, 20%, 30%, 40%, 50%, 55% and 60% of the ultimate value.

##### 4.2. Design of PZTs layer

Based on the concept of smart layer<sup>[9]</sup>, the PZTs layer is developed to be convenient for placing the PZT network on large scale structures and to ensure each PZT within the network has the same actuating and sensing properties. The cross section and designed PZTs layer are shown in Fig.8. Three main design points are considered:

(1) Based on the sensor interface of scanning module, the input/output interface of PZTs layer is designed as shown in Fig.8(b).

(2) 11 PZTs are placed as a linearly uniform array on PZTs layer. Depending on the requirement of monitoring task, it can be trimmed at will or used as a whole.

(3) The substrate layer of PZTs layer shown in Fig.8(a) is polyimide film. It is durable and thin (125 μm thick). This kind of material can ensure long service life of PZTs layer and bring about low effect on monitored structures.

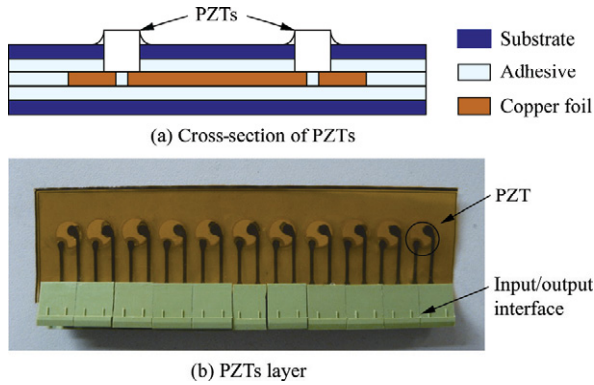
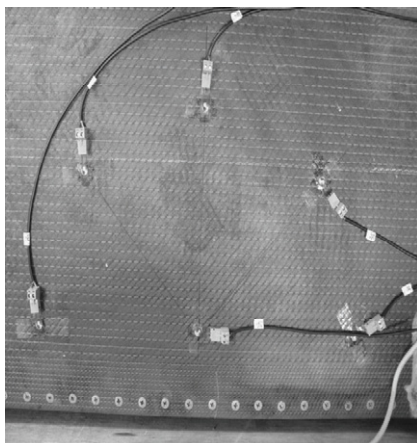


Fig.8 PZTs layer designed for experiment.

4.3. Selection of excitation frequency

In this section, one PZTs layer is trimmed to be containing individual PZT. Seven PZTs are placed on the outer surface of upper panel to form a PZT network as shown in Figs.9(a)-9(b). PZTs 1, 2 and 6 are placed along the 0° direction of the material wearing pattern. The PZT network is connected with PXI-ISS by shielded wires.

Five actuator-sensor channels (1-2, 1-3, 1-4, 1-5, 1-6) are defined. To verify the function of single channel frequency scanning of PXI-ISS, the scanning frequencies which are between 30 kHz and 450 kHz (with 10 kHz interval) are adopted for each channel to search the best excitation frequency for this kind of wing box. The amplitude of frequency scanning signal is ±80 V. Fig.9(c) shows the response signals of 30 kHz to 100 kHz acquired from channel 1-2. They give that the wave packets of the response signals are clearer and the amplitude of them are higher between 30 kHz and 50 kHz relative to that for other frequencies. Fig.9(d) shows the corresponding frequency spectra. It describes that the energy of signals between 30 kHz and 50 kHz are more compact and the frequency dispersion is lower. The results of the other channels are similar. So in this article, the frequency range is selected as 30 kHz to 50 kHz to be the central frequency of the excitation signal in the following research.



(a) Wing box

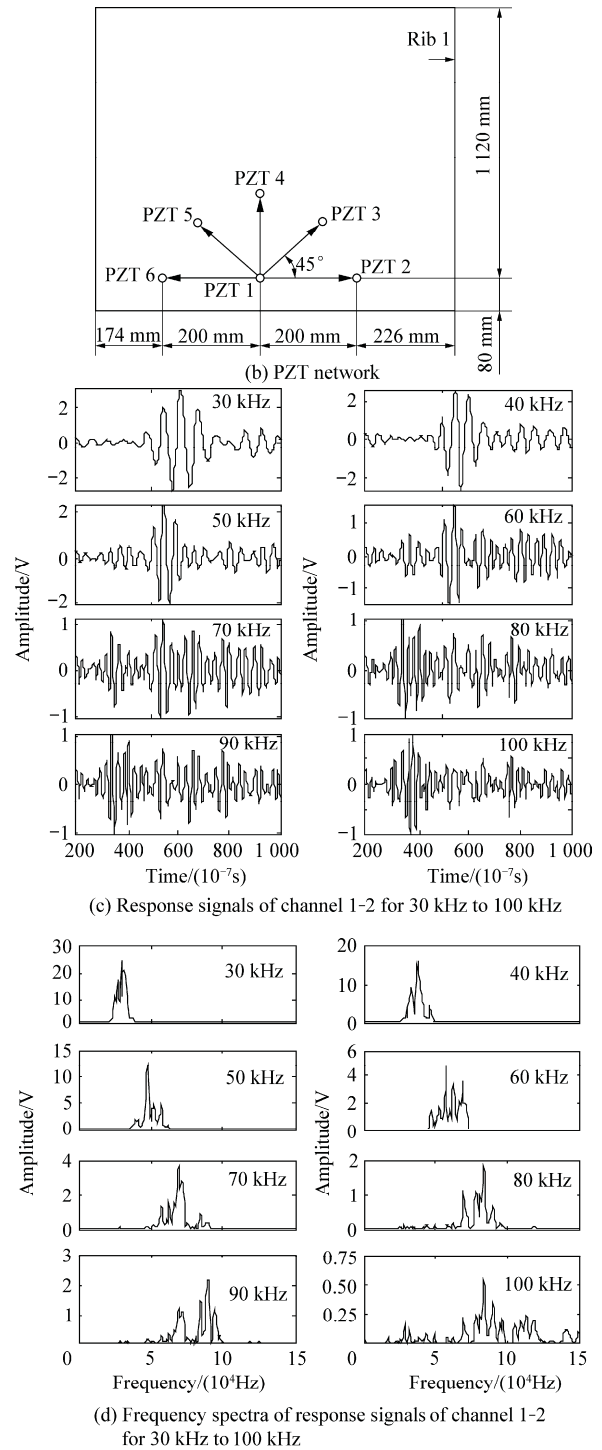


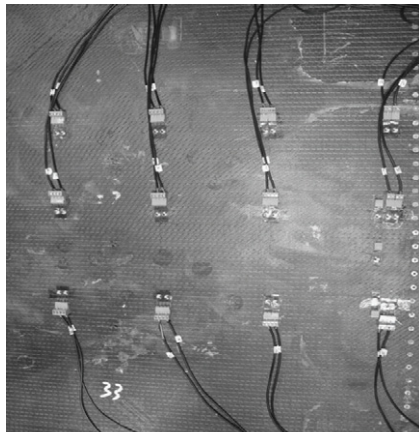
Fig.9 PZT network and response signals of selected frequencies.

4.4. Simulating damage imaging

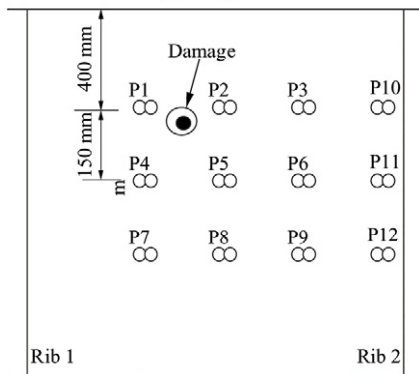
In this section, the PZTs layers are trimmed to be PZT pairs. They are placed on the outer surface of upper panel to form a PZT network as shown in Fig.10(a). In Fig.10(b), every PZT pair is adopted to form an actuator-sensor pair. Six monitoring areas are constructed by 12 actuator-sensor pairs. Every four adjacent pairs construct a monitoring area, which contains 12 actua-

tor-sensor channels. There are totally 72 actuator-sensor channels being defined. The space between the two PZTs of each pair is 2 mm. The space between the actuator-sensor pair is 150 mm. To avoid the boundary reflections, the monitoring areas are far from the structural boundary. PZTs are connected with PXI-ISS by shielded wires.

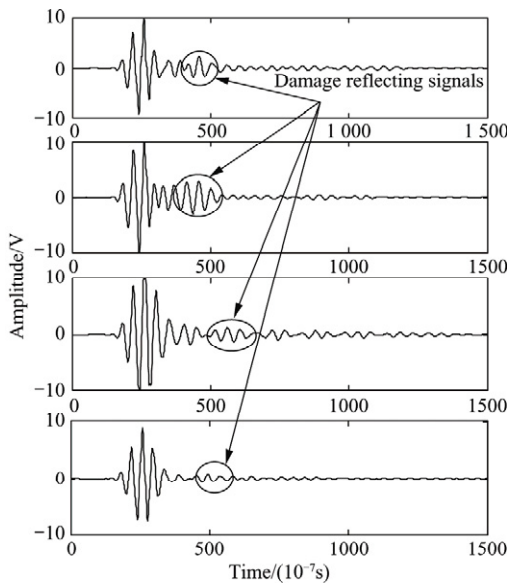
The 72 channels are scanned in order using the function of multi-channel scanning of PXI-ISS. The frequency and amplitude of excitation signal are 30 kHz



(a) Wing box



(b) PZT network and damage



(c) Response signals of P1, P2, P4 and P5

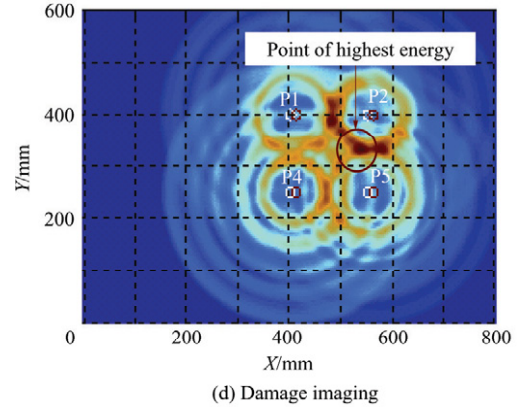


Fig.10 PZT network and monitoring results.

and  $\pm 80$  V. A weight of 200 g is adhered in monitoring area to simulate the damage. Fig.10(b) shows its location. Fig.10(c) gives the response signals acquired from the actuator-sensor pairs P1, P2, P4 and P5 respectively. The damage introduces reflecting signals into each response signal. But small boundary reflecting signals also exist next to the damage reflecting signals just as shown in Fig.10(c). Fig.10(d) shows the imaging of the damage using time reverse method. The highest area of image energy has some bias against the actual damage position. Considering the complicated dispersion nature of Lamb wave caused by CFRP materials which makes the wave group velocity be different in each direction, this result can be accepted.

4.5. Stability test of PXI-ISS

Fig.11 gives the arrangement of rib-bolts on the two ribs and the arrangement of PZT network on the inner surface of the upper panel. The PZTs are connected with PXI-ISS by shielded wires.

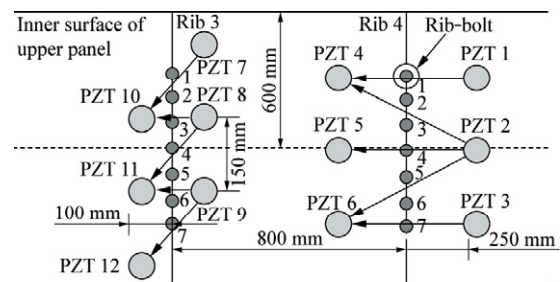


Fig.11 Arrangement of rib-bolts and PZT network.

Fig.12 displays the response signals acquired seven times from actuator-sensor channels 2-4 and 2-5 respectively under the set load of 30% at different time. It shows that these signals are almost the same. The maximum relative errors of the peak values with respect to  $\pm 10$  V sampling range are 0.04% and 0.05% respectively. These results demonstrate the good stability of PXI-ISS.

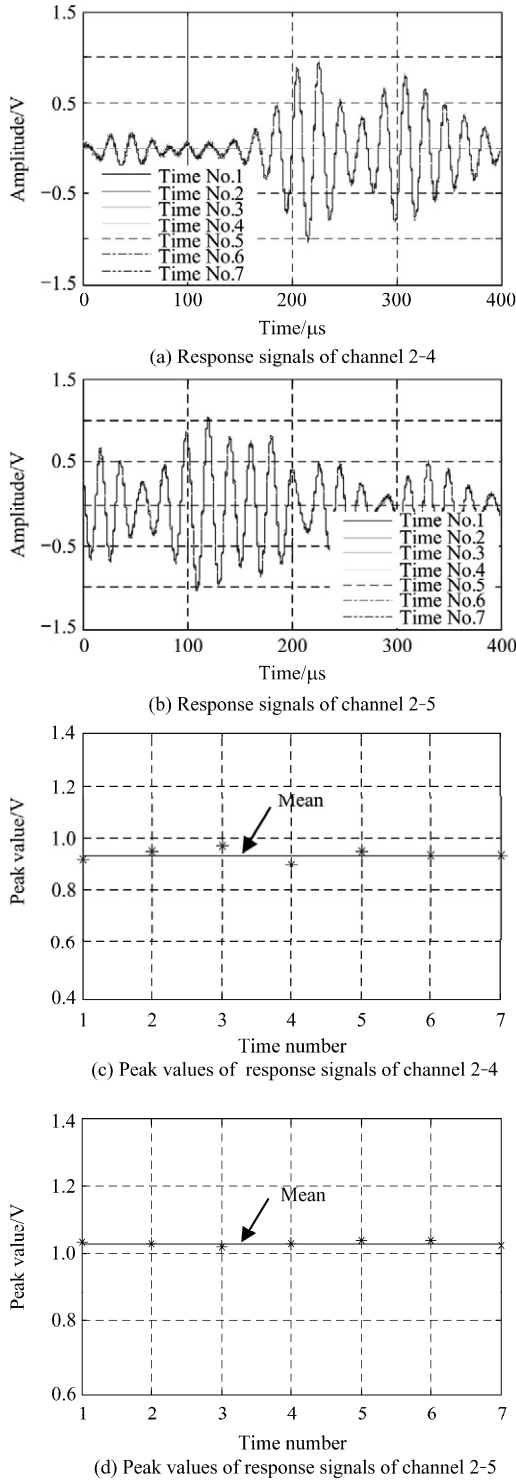


Fig.12 Seven response signals of channels 2-4 and 2-5.

4.6. Loading effect on signals

Loading makes the wing box be deformed and affects the propagation of Lamb wave signals. Fig.13 displays the response signals acquired from channel 2-5 under the loading set from 0% to 60%. Fig.13 shows that the stability of the response signals is worse than that of the response signals shown in Fig.12. The maximum relative error is 0.1%. But the load nearly

does not change the time of the peak values of response signals, so the features of the time-of-flight of the response signals are not changed. The load also leads the energy of the whole signals to be increased or decreased, but the damages just as shown in Fig.10 only introduce reflecting signals into the part of the response signals. In these cases, the main characteristics of the response signals are not changed by the load.

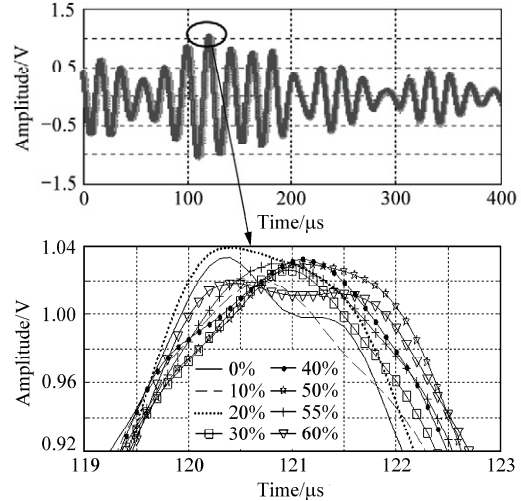


Fig.13 Response signals of channel 2-5 at each set load.

5. Conclusions

This article presents an active Lamb wave and PZT network based multi-channel scanning system. Both hardware and software are designed and developed. The results of the ground-based experiment have shown its satisfactory performance.

5.1. Specifications of PXI-ISS

The basic operating parameters of PXI-ISS are: ① physical dimensions: 280 mm  $\times$  177 mm  $\times$  303 mm ( $W \times H \times D$ ); ② signal generation: programmable arbitrary waveform generator and adjustable amplitude and frequency for waveform output; ③ transmission/receiving frequency: 15 kHz to 640 kHz bandwidth; ④ power gain: fixed 10 times of gain and  $\pm 80$  V maximum output; ⑤ signal gain: 4 channels programmable gains and sensitivity; ⑥ data acquisition: 4 channels high signal acquisition speed up to 10 MHz with low cross talk signal; ⑦ PZT network: supporting up to 3 PZT networks; ⑧ PZT channels per network: supporting up to 24 PZTs and 276 unrepeatable actuator-sensor channels; and ⑨ all these parameters are expandable.

This system includes the following main features: ① it is compact, portable and easy to fix; ② it can scan large numbers of actuator-sensor channels or can accomplish one channel frequency scanning task; ③ the on-line SHM task can be accomplished by it, because it can process response signals and assess

damage automatically; ④ it has a uniform software system which is easy to be used and expanded; and ⑤ it can be applied to conducting general PZT network-based experiment or on-line damage assessment.

### 5.2. Future research

Considering the dispersion nature of Lamb wave in structures, the mode analysis modules and wave group velocity compensation methods should be integrated into the system software to improve the precision of damage assessment. How to reduce the boundary reflecting signals to enlarge monitoring area should also be considered.

In the follow-up research for improving PXI-ISS, the above-mentioned two issues, more details about damage assessment methods and assessing different kinds of practical damage patterns will be discussed.

### References

- [1] Yuan S F. Structural health monitoring and damage control. 1st ed. Beijing: National Defence Industry Press, 2007.[in Chinese]
- [2] Giurgiutiu V. Tuned Lamb wave excitation and detection with piezoelectric wafer active sensors for structural health monitoring. *Journal of Intelligent Material Systems and Structures* 2005; 16(4): 291-305.
- [3] Rguiti M, Grondel S, El Youbi F, et al. Optimized piezoelectric sensor for a specific application: detection of Lamb waves. *Sensors and Actuators: A, Physical* 2006; 126(2): 362-368.
- [4] Peng G, Yuan S F, Xu X. Damage detection on two-dimensional structure based on active Lamb waves. *Smart Structures and Systems* 2006; 2(2): 171-188.
- [5] Zhao X, Gao H, Zhang G, et al. Active health monitoring of an aircraft wing with embedded piezoelectric sensor/actuator network: I, defect detection, localization and growth monitoring. *Smart Materials and Structures* 2007; 16(4): 1208-1217.
- [6] Lee B C, Staszewski W J. Sensor location studies for damage detection with Lamb waves. *Smart Materials and Structures* 2007; 16(2):339-408.
- [7] Raghavan A, Cesnik C E S. Review of guided-wave structural health monitoring. *The Shock and Vibration Digest* 2007; 39(2): 91-114.
- [8] Yuan S F, Liang D K, Shi L H, et al. Recent progress on distributed structural health monitoring research at NUA. *Journal of Intelligent Material Systems and Structures* 2008; 19 (3): 373-386.
- [9] Lin M, Qing X, Kumar A, et al. Smart layer and smart suitcase for structural health monitoring application. *Proceedings of SPIE: Smart Structures and Materials*. 2001; 4332: 98-106.
- [10] Qing X, Chan H, Bread S J, et al. An active diagnostic system for structural health monitoring of rocket engines. *Journal of Intelligent Material Systems and Structures* 2006; 17(7): 619-628.

- [11] Dove J R, Park G, Farrar C R. Hardware design of hierarchical active-sensing networks for structural health monitoring. *Smart Materials and Structures* 2006; 15(1): 139-146.
- [12] Liu W, Giurgiutiu V. Automation of data collection for PWAS-based structural health monitoring. *Proceedings of SPIE: Smart Structures and Materials*. 2005; 5756: 1139-1147.
- [13] Jenkins C, Giurgiutiu V, Lin B, et al. Development of specifications for an integrated piezoelectric wafer active sensors system. *Proceedings of SPIE: Smart Structures and Materials*. 2005; 5764: 509-521.
- [14] Qiu L, Yuan S F. Research and application of integrated health monitoring scanning system based on PZT sensor array. *Piezoelectrics & Acoustooptics* 2008; 30(1): 39-41, 44.[in Chinese]
- [15] Wang Q, Yuan S F, Qiu L. Study on bolt debonding monitoring of composite joint based on time-reversal method. *Journal of Astronautics* 2007; 28(6): 1710-1723.[in Chinese]

### Biographies:

**Qiu Lei** Born in 1983, he received B.S degree from Nanjing University of Aeronautics and Astronautics in 2006. Now he is a Ph.D. candidate in this university. His main research interests are test instrument, artificial intelligent, sensor technology, signal processing, mechanical analysis and modeling, and structural health monitoring application research. E-mail: ql19830925@nuaa.edu.cn

**Yuan Shenfang** Born in 1968, she received B.S., M.S. and Ph.D. degrees from Nanjing University of Aeronautics and Astronautics. Her main research interests are smart materials and structures, signal processing, intelligent monitoring and intelligent wireless sensor network, etc. E-mail: ysf@nuaa.edu.cn

**Wang Qiang** Born in 1980, he received M.S. degree from Nanjing University of Aeronautics and Astronautics in 2005. Now he is a Ph.D. candidate in this university. His main research interests are structural health monitoring, sensor and measurement technology, signal processing methods and information processing methods. E-mail: wq21cn@nuaa.edu.cn

**Sun Yajie** Born in 1980, she received M.S. degree from Nanjing University of Aeronautics and Astronautics in 2005. Now she is a Ph.D. candidate in this university. Her main research interests are structural health monitoring, sensor technology, signal processing and information fusion. E-mail: sunyajie@nuaa.edu.cn

**Yang Weiwei** Born in 1985, she received B.S. degree from Nanjing Normal University in 2007. Now she is a M.S. candidate in Nanjing University of Aeronautics and Astronautics. Her main research interests are structural health monitoring, FPGA&DSP-based system development and sensor technology. E-mail: yww222@nuaa.edu.cn